Chapter 8

Antarctic Ice Sheet dynamics during the Late Oligocene and Early Miocene: climatic conundrums revisited

Tim R. Naish[1], Bella Duncan[1], Richard Levy[1,2], Robert M. McKay[1], Carlota Escutia[3], Laura De Santis[4], Florence Colleoni[4], Edward G.W. Gasson[5], Robert M. DeConto[6] and Gary Wilson[2]

[1]Antarctic Research Centre, Victoria University of Wellington, Wellington, New Zealand, [2]GNS Science, Lower Hutt, New Zealand, [3]Andalusian Institute of Earth Sciences, CSIC and Universidad de Granada, Armilla, Spain, [4]National Institute of Oceanography and Applied Geophysics – OGS, Sgonico, Italy, [5]School of Geographical Sciences, University of Bristol, Bristol, United Kingdom, [6]Department of Geosciences, University of Massachusetts, Amherst, Amherst, MA, United States

8.1 Introduction

Investigating the drivers of ice volume change in the geological past has been a primary goal of the Scientific Committee on Antarctic Research (SCAR) Past Antarctic Ice Sheet (PAIS) Dynamics strategic research programme. These drivers include: (1) millennial-scale variations in local insolation, atmosphere and ocean forcing caused by quasi-periodic changes in Earth's orbital parameters ('Croll-Milankovitch cycles'), (2) longer-term, million-year trends controlled by more gradual changes in atmospheric greenhouse gas concentrations (e.g., Masson-Delmotte et al., 2013; Zhang et al., 2013), and (3) slowly-evolving plate tectonic changes modulating ocean currents and the flow of heat around Antarctica (Bijl et al., 2013; Kennett, 1977; Kennett et al., 1974; Sijp et al., 2014), as well as impacting the topography and elevation of the continent (Paxman et al., 2019, 2020; Wilson and Luyendyk, 2009).

The Late Oligocene to Early Miocene (~26–22 Ma) is an important period of Earth history during which the Antarctic Ice Sheet (AIS) was

Antarctic Climate Evolution. DOI: https://doi.org/10.1016/B978-0-12-819109-5.00013-X

highly dynamic. Here, we use it to examine the relative influences of plate tectonics, atmospheric carbon dioxide and orbital forcing on southern high-latitude regional climate and the evolution of the ice sheet. We provide a synthesis of the latest research as an update on the first edition of this chapter, which focussed primarily on the role of orbital forcing on ice sheet variability (Wilson et al., 2009). Our approach summarises the latest and most complete reconstructions of geography and bathymetry, Southern Ocean and atmospheric temperature, atmospheric carbon dioxide, and Antarctic ice volume and its influence on global sea level, using geological proxies from locations in the near and far-field of the AIS (Fig. 8.1).

This chapter presents some major advances over the last 10 years, and also highlights some remaining challenges that still hamper reconstructions, and a better understanding of Earth's climate system using geological proxies. These include:

1. Cenozoic atmospheric CO_2 compilations reconstructed from alkenone and boron have limited resolution (Badger et al., 2013; Pagani et al., 2005, 2010, 2011; Seki et al., 2010; Super et al., 2018; Zhang et al., 2013) and boron (Bartoli et al., 2011; Foster et al., 2012; Greenop et al., 2014, 2019; Honisch et al., 2009; Martinez-Boti et al., 2015) proxies. This is especially true during the Oligocene and Miocene, where the relationship between longer-term secular variation on millions of year timescales and shorter-term millennial-scale fluctuations in the carbon cycle are difficult to reconcile (e.g., Greenop et al., 2019).
2. Deep-ocean benthic foraminiferal $\delta^{18}O$ records provide the most detailed proxy for long-term and glacial-interglacial climate variability during the Cenozoic (e.g., Cramer et al., 2009; De Vleeschouwer et al., 2017; Westerhold et al., 2020; Zachos et al., 2001a). However, deconvolving the relative influence of ocean temperature and ice volume on $\delta^{18}O$ composition is not straight forward. It is generally accepted that prior to the development of continental scale ice sheets across Northern Hemisphere continents, which began $\sim$3 Ma, the Cenozoic benthic $\delta^{18}O$ record reflects predominantly Antarctic ice volume and bottom-water temperature. Although these two properties typically co-vary, they appear to decouple in the Late Oligocene (e.g., Greenop et al., 2019; Hartman et al., 2018; Hauptvogel et al., 2017; Pekar et al., 2006).
3. To address this, several studies have used paired Mg/Ca paleothermometry, on the same foraminiferal calcite used in benthic $\delta^{18}O$ records, to extract the temperature component (e.g., Cramer et al., 2009; Lear et al., 2015; Miller et al., 2020; Shevenell et al., 2008). Unfortunately, most of these records are restricted to mid- and low-latitude sites, because of the poor-preservation of calcitic-microfossils in the cold CO_2 saturated waters of the Southern Ocean. Moreover, this method contains significant uncertainties outlined in detail by Raymo et al. (2018). Recently, upper Southern Ocean

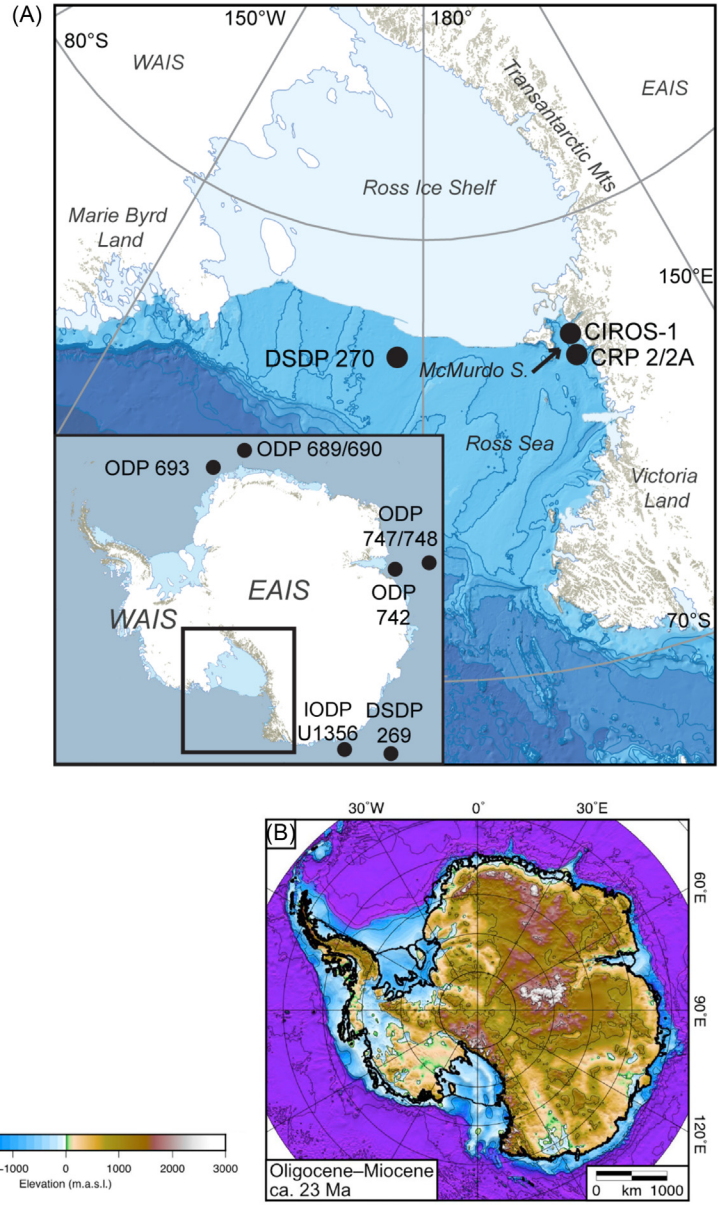

FIGURE 8.1 (A) Location map of present day Ross Sea sector and Antarctica (inset) showing drill sites and locations referred to in the text. (B) Reconstructed topography for the Oligocene-Miocene Transition. The elevations are given relative to present-day mean sea level, and contoured at 1 km intervals. Note that elevations are for fully isostatically-relaxed ice-free conditions. *Reproduced from Paxman et al. (2019).*

temperatures have been derived from sediment cores on the Antarctic continental margin using glycerol dialkyl glycerol tetraethers (GDGTs), membrane lipids formed by archaea and some bacteria (e.g., Hartman et al., 2018; Levy et al., 2016; Sangiorgi et al., 2018). Significant advances in assessing the drivers of long-term AIS volume change from the benthic $\delta^{18}O$ record are now being made through the development of independent records of high-southern latitude ocean temperature through the use of lipid biomarkers (e.g., Hartman et al., 2018; Sangiorgi et al., 2018).

4. Alternatively, ice volume calibrations of the benthic $\delta^{18}O$ record have been constrained using sea-level reconstructions from back-stripped continental margins (shallow marine sedimentary sequences that have tectonic, isostatic and compaction effects removed; e.g., Cramer et al., 2011; Grant et al., 2019; Miller et al., 2005, 2020; Kominz et al., 2008; Pekar and Kominz, 2001), but the accuracy is often hampered by the limited precision of paleodepth indicators and the influence of sediment erosion during sea-level lowstands, leading to underestimation of the full amplitude of sea-level change.
5. Antarctic paleogeographic reconstructions show that the morphology of the bedrock surface has evolved substantially over the past 34 million years. At the Eocene-Oligocene Transition (see Galeotti et al., 2016), most of the West and East AISs formed on a land surface above sea level (De Santis et al., 1999; Hochmuth et al., 2020; Paxman et al., 2019, 2020; Wilson and Luyendyk, 2009). With time, tectonic subsidence, sediment erosion, and ice and water loading have resulted deepening of many previously emergent sectors of the Antarctic margin (and that are situated below sea-level today). These paleogeographic reconstructions, together with the timing of subsidence, have significant implications for understanding the evolution of the AIS. It is much easier to grow an ice sheet on land than on a submarine bed. For example, continental-scale dynamic ice sheet modelling studies, that use restored Antarctic paleogeography for the Oligocene and Miocene, show West Antarctica accommodated a much larger reservoir of ice than today, even when ocean temperatures in the Ross Sea were relatively warm (e.g., Colleoni et al., 2018; Gasson et al., 2016; Paxman et al., 2020; Wilson et al., 2013). Marine-based ice is inherently more sensitive to ocean warming than atmospheric heat, and retreat is exacerbated by non-linear processes such as marine ice sheet instability on reverse-slope bed topography and/or marine ice cliff instability if ice shelves disintegrate (DeConto and Pollard, 2016; Gasson et al., 2016; Pollard et al., 2015), due primarily to incursions of warm water toward and at ice sheet grounding lines (e.g., Levy et al., 2019).

8.2 Oligocene-Miocene Transition in Antarctic geological records and its climatic significance

Early definition of the Oligocene-Miocene Transition (OMT) relied on the identification of the last occurrence of the calcareous nannofossil

Dictyococcites bisectus (23.7 Ma; Berggren et al., 1985). However, the use of this stratigraphic marker proved problematic in the colder waters, coarse sediments and hiatus prone strata of the Antarctic and Southern Ocean. The reassignment of the Epoch boundary by Cande and Kent (1992, 1995) to the slightly older base of Magnetic Polarity subchron C6Cn.2n (23.8 Ma; Fig. 8.2) made its identification more straightforward in Antarctica and the Southern Ocean, but only in relatively complete and continuous stratigraphic successions (e.g., Kulhanek et al., 2019; Roberts et al., 2003; Wilson et al., 2002). More recently, the recognition of astronomically-influenced cyclical physical properties, and $\delta^{18}O$ records in continuously deposited deep successions, has enabled astronomical calibration of Late Oligocene through Early Miocene time. The astronomical calibration suggested that, while still coincident with the base of subchron C6Cn.2n, the boundary was in fact nearly a million years younger (22.9 ± 0.1 Ma; Pälike et al., 2004; Shackleton et al., 2000; 23.03 Ma; Billups et al., 2004; Gradstein et al., 2004; Fig. 8.2).

The climatic significance of this was outlined by Zachos et al. (1997, 2001a,b) and Pälike et al. (2006) who recognised the coincidence of the OMT with the culmination of a $\sim$300 kyr-duration, up to $\sim +1‰$, $\delta^{18}O$ excursion (Mi-1 event; Miller et al., 1991) with a $\sim$1.2 myr low-amplitude variability in the eccentricity and obliquity of the Earth's orbit (Fig. 8.2). An attempt to constrain the ice volume component of the Mi-1, $\delta^{18}O$ excursion using the global sea-level estimates from the New Jersey continental margin (Pekar et al., 2006), implied the AIS may have grown to 120% of its present-day size, which should be regarded as a maximum as these estimates are uncorrected for glacio-isostatic adjustment (GIA) and contain large uncertainties (discussed above). Notwithstanding this, the New Jersey records appear to be consistent with estimates from numerical ice sheet simulations using reconstructed paleotopographies, $\sim$300 ppm atmospheric CO_2, and cold orbits run to equilibrium (Gasson et al., 2016; Wilson et al., 2002).

Levy et al. (2019), using an analysis of the most recent $\delta^{18}O$ compilation for the Cenozoic (De Vleeschouwer et al., 2017), identified a progressive increase in the obliquity sensitivity parameter (S_{obl}) between 24.5 and 23.5 Ma and associated this with a significant period of AIS growth. Indeed, using proximal geological evidence, Levy et al. (2019) showed that the Mi-1 glaciation was the first major expansion of ice sheets across the Ross Sea continental shelf since the Eocene-Oligocene Transition and the onset of Antarctic glaciation (e.g., Galeotti et al., 2016). This was based on the first occurrence of ice proximal glacimarine sediments in the DSDP Site 270 (Kulhanek et al., 2019) and disconformities in Cape Roberts Project (CRP) site CRP-2/2A (Naish et al., 2001). Further evidence for continent-wide glacial expansion and climatic deterioration comes from the occurrence of mass transport deposits (MTDs) on the continental rise at International Ocean Discovery Program (IODP) Site U1356 in the Wilkes Land region (Escutia et al., 2011, 2014), alongside a large turnover in Southern Ocean phytoplankton (Crampton et al., 2016) and Antarctic

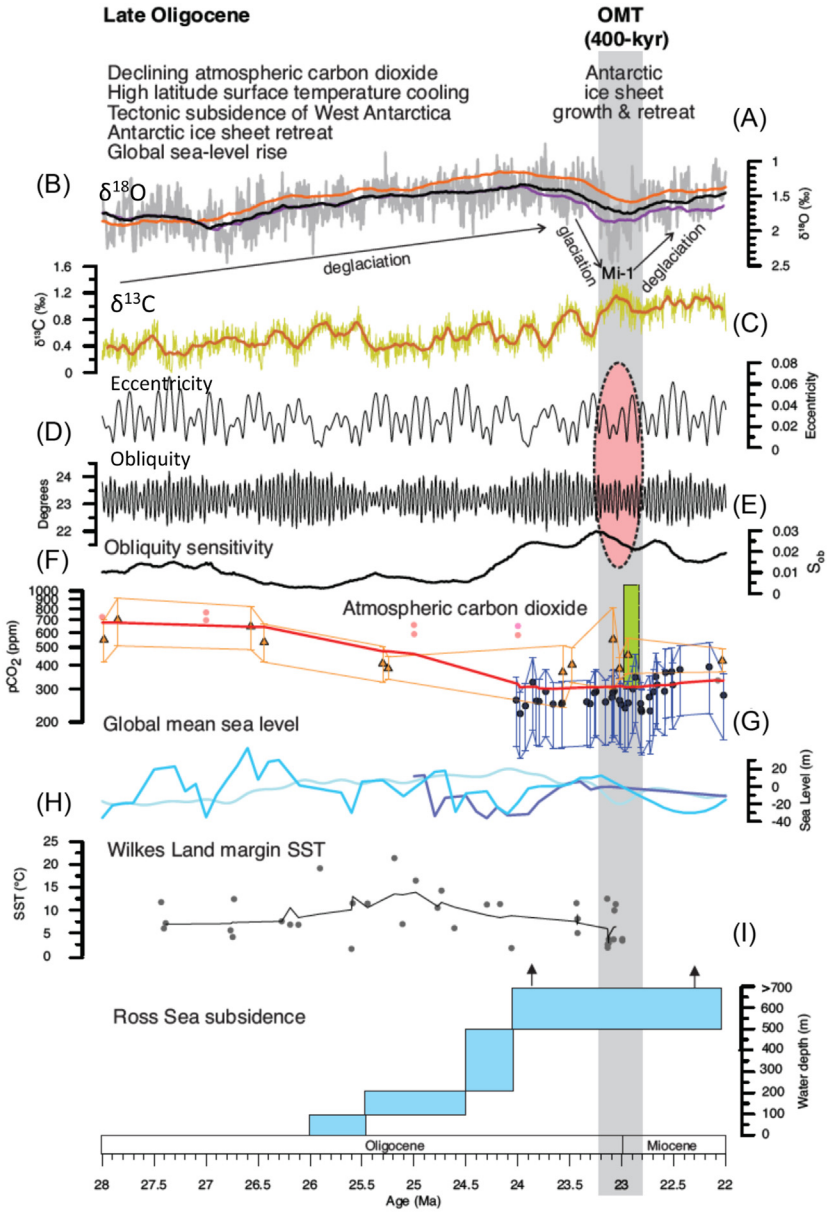

FIGURE 8.2 Late Oligocene and Oligocene-Miocene climate Transition (OMT). (A) Smoothed 500-kyr moving averages of benthic foraminiferal $\delta^{18}O$ stacks from Cramer et al. (2009), De Vleeschouwer et al. (2017) and Miller et al. (2005), superimposed on the high resolution benthic $\delta^{18}O$ record of Liebrand et al. (2011). (B) Benthic foraminiferal $\delta^{13}C$ record from Liebrand et al. (2011). (C) Eccentricity and (D) obliquity forcing (Laskar et al., 2004). (E) Obliquity sensitivity in

(*Continued*)

shelf-wide unconformities in seismic data (De Santis et al., 1995; Donda et al., 2008; Escutia et al., 1997, 2005; Mckay et al., 2021; Sorlien et al., 2007) (Fig. 8.1).

A reassessment of the chronostratigraphy of Deep Sea Drilling Project (DSDP) Site 270 in the Ross Sea (Kulhanek et al., 2019) provides the most complete ice proximal stratigraphic record of the Oligocene-Miocene boundary in Antarctica. It is correlated with an interval of mudstone containing ice-berg rafted debris between 149 and 146 m below sea-floor (mbsf), but may potentially fall within an ~100-kyr-duration unconformity at 149 mbsf. The boundary occurs ~70 m above grounding-line proximal diamictite, sandstone and laminated mudstone, raising questions about the additional role of hydro-glacio-isostatic adjustment (GIA) on near-field sea-level change at this time. In the even more ice-proximal CRP-2A core adjacent to the Victoria Land coast the OMT and the majority of the preceding Mi-1, $\delta^{18}O$ excursion is missing within a ~3 Myr-duration unconformity at the base of Sequence 8 (Naish et al., 2008). Roberts et al. (2003) placed the OMT at 274 m in the CIROS-1 core, ~35 km south of CRP-2A (Fig. 8.1), within an interval of ice-proximal glacimarine diamictite. However, following the relocation of the original position of OMT (e.g., Wilson et al., 2002) by Naish et al. (2008), it is also missing in the CIROS-1 core and most likely correlates with an unconformity at 92 m (Wilson et al., 2009).

Ice-distal, Late Oligocene-Early Miocene strata reported from the East Antarctic margin include Maud Rise (ODP Leg 113 Sites 689 and 690; Barker et al., 1999), the Weddell Sea margin (ODP Leg 113 Site 693; Barker et al., 1999) and Kerguelen Plateau (ODP Leg 120 sites 747 and 748; Fraass et al., 2019; Schlich and Wise, 1992; Fig. 8.1). The record at Maud Rise is relatively thin and comprises exclusively siliceous and carbonate ooze, although rare glacial dropstones are reported in strata from Site 689 (Barker et al., 1999). In the Weddell Sea margin, Oligocene-Miocene sediments are also fine-grained and include diatom mud, clay and ooze (Barker et al., 1988). OMT sediments at Kerguelen Plateau are also carbonate ooze (Schlich and Wise, 1992). Foraminifera preservation and age resolution were good enough at ODP Site 747 to yield a benthic oxygen isotope stratigraphy across the boundary at that site (Billups and Schrag, 2002; Wright and Miller, 1992), although a recent re-

◀ the benthic $\delta^{18}O$ stack of De Vleeschouwer et al. (2017), calculated by Levy et al. (2019) and considered to represent the relative presence of marine-based AISs. (F) Atmospheric CO_2 (red line is median) reconstructed from alkenones (orange triangles; Pagani et al., 2011; Zhang et al., 2013), boron (black dots; Sosdian et al., 2018; Greenop et al., 2019), phytane (pink dots, Witkowski et al., 2018), and stomatal gas exchange method (green box; Reichgelt et al., 2016). (G). Global mean sea-level reconstructed from sequence stratigraphic back-stripping of the New Jersey continental margin (Cramer et al., 2011; Kominz et al., 2008; Miller et al., 2020). (H) Near surface ocean temperature off Wilkes Land, Antarctica (Hartman et al., 2018). (I) Water depth estimates from DSDP Site 270, Ross Sea, Antarctica (Leckie and Webb, 1983; Kulhanek et al., 2019).

evaluation of the age model and new benthic oxygen isotope stratigraphy suggests that the OMT occurs within a ~200 kyr unconformity (Fraass et al., 2019). The amplitude of the Mi-1 event was much reduced compared to equatorial values, with a $\delta^{18}O$ shift of only 0.3‰ across the OMT.

Drilling on the East Antarctic margin in Prydz Bay (ODP Legs 119 and 188; Cooper and O'Brien, 2004; Hambrey et al., 1991) did not yield any Late Oligocene-Miocene age strata and Hambrey et al. (1991) concluded that this was due to erosion beneath an expanded middle Miocene ice sheet. Seismic stratigraphy on the inner continental shelf across the Prydz Channel to the shallow outer shelf, that intersects with ODP drill sites, shows widespread erosion that correlates with a probable Late Oligocene-Early Miocene stratigraphic hiatus at the drill Site ODP 742 (Mckay et al., 2021). While, this does not provide unequivocal evidence of large-scale grounding of a marine-based ice sheet after that time, it does suggest ice advanced into fjords and across the shallow continental shelf during, or after, the OMT (Barron and Larsen, 1989; Hambrey et al., 1991; Mckay et al., 2021). Although the OMT interval was not directly sampled, marine geological and geophysical data from the continental shelf seaward of the Aurora subglacial basin Gulick et al. (2017) infer that grounded ice advanced across, and retreated from, the Sabrina Coast continental shelf at least 11 times during the Oligocene and Miocene epochs.

At Site U1356, located in ~4 km of water depth adjacent to the East Antarctic Wilkes Land margin, the OMT overlies a poorly recovered interval of alternations of laminated and bioturbated diatomaceous contourites and sediment gravity flow deposits, punctuated by Mass Transport Deposits (MTDs) and numerous hiatuses (Escutia et al., 2011; 2014). The OMT is associated with a dramatic change in depositional style on the Wilkes Land margin from MTD-dominated to turbidite/contourite dominated deposition (Escutia et al., 2011; 2014; Tauxe et al., 2012). TEX_{86} records show cooling from 25 to 23 Ma with lowest temperatures coincident with the OMT (Hartman et al., 2018; Fig. 8.2). Sedimentological and geochemical indicators, dinocyst associations and SST variations point to a dynamic oceanic frontal system paced by glacial-interglacial climate variability across the OMT (Bjil et al., 2018; Hartman et al., 2018; Salabarnada et al., 2018).

A recent reassessment of the chronostratigraphy of DSDP Leg 28, Site 269, located on the abyssal plain ~280 km seaward from Site U1356, revealed sediments dated ~24.2 to ~23 Ma (Evangelinos et al., 2020). Although the site was not continuously cored, the recovered sediments contain the record that was interrupted by MTD deposits at Site U1356, thus providing snapshots into the oceanic conditions that prevailed in this sector of the Southern Ocean when ice sheets were expanding repeatedly onto the Wilkes Land continental shelf during the latest Oligocene. Evangelinos et al. (2020) imply that overall cooling and ice sheet advance was punctuated by

warm interglacials associated with enhanced upwelling of Circumpolar Deep Water (CDW) as the polar front episodically migrated southward.

8.3 Conundrums revisited

8.3.1 What caused major transient glaciation of Antarctica across the OMT?

The OMT is characterised by up to +1‰ cooling event that occurs as a two-step increase in benthic foraminiferal $\delta^{18}O$ over 200−300 kyr (Mi-1 glaciation of Miller et al., 1991), followed by a dramatic two-step rebound of −1.2‰ within 100 kyr (e.g., Liebrand et al., 2011; 2016; 2017; Fig. 8.2). Although it is not possible to discount a Northern Hemisphere ice contribution (e.g., DeConto et al., 2008), the OMT has been widely attributed to expansion and collapse of the AIS, driving changes in global mean sea-level of between 30 and 90 m (Greenop et al., 2019; Kominz et al., 2008; Liebrand et al., 2011; Levy et al., 2019; Mawbey and Lear, 2013; Miller et al., 1991, 2005, 2020; Naish et al., 2001; Pälike et al., 2006; Paul et al., 2000; Pekar et al., 2002).

The entire OMT spans a 400-kyr eccentricity cycle. Numerous studies have noted the coincidence of the glacial phase (Mi-1 glaciation) with a 1.2-Myr-paced minimum in the modulation of the Earth's axial tilt (an obliquity node), as well as a minimum in the 400-kyr-long eccentricity cycle (a very circular orbit), which together favour lower mean annual insolation and lower seasonality, conducive to ice sheet growth (Coxall et al., 2005; Pälike et al., 2006; Zachos et al., 2001a) (Fig. 8.2). While obliquity variance was low, the AIS appeared to be highly responsive to ice volume variability in the obliquity band (Naish et al., 2001; Levy et al., 2019). This heightened 'obliquity sensitivity' (S_{obl}) (Fig. 8.2) was attributed to the first major expansion of the AIS into the ocean, as near-surface temperatures cooled through a threshold, whereby marine-based ice could be sustained on the continental shelf. Both Naish et al. (2009) and Levy et al. (2019) have argued that the mass balance of marine-based ice sheets is modulated by obliquity via its influence on the pole-equator temperature gradient controlling the upwelling of CDW (e.g., Toggweiler et al., 2007), with consequences for melt rates at marine grounding lines.

However, Greenop et al. (2019) observed that the obliquity nodes and eccentricity minima occur regularly throughout the Late Oligocene (Laskar et al., 2004; Pälike et al., 2006) and the amplitude of the preceding node at 24.4 Ma is more extreme than the one associated with the OMT (Fig. 8.2). This is also consistent with strong orbital modulation of proximal glacimarine sedimentation in the Ross Sea (Naish et al., 2001), and SSTs and ocean dynamics on the Wilkes Land margin prior to the OMT, as discussed above (Bjil et al., 2018; Evangelinos et al., 2020; Hartman et al., 2018; Salabarnada et al., 2018).

On this basis, Greenop et al. (2019) proposed the additional role of a long-term decline in atmospheric CO_2, which dipped below 400 ppm for the first time in the Cenozoic (Fig. 8.2), cooling the climate to a state whereby an extreme orbital configuration could trigger widespread Antarctic glaciation and the development of the first marine-based ice margins. A similar CO_2 threshold of ~400 ppm for marine-based ice sheet development had been proposed by Foster and Rohling (2013) based on the empirical relationship between global ice volume and atmospheric CO_2 in proxy records, and by Naish et al. (2009) and Levy et al. (2016; 2019) based on direct geological evidence from Antarctic margin drill cores.

The AIS expansion had a dramatic effect on Southern Ocean sea surface temperatures and sea ice extent via the influence of albedo on regional temperatures and its elevation on low-level winds. Numerical climate and ice sheet simulations clearly show that a growing Mi-1 ice sheet cooled Southern Ocean sea surface temperatures by several degrees, pushing the 0°C isotherm equatorward and increasing the area, thickness and concentration of seasonal and perennial sea ice cover (DeConto et al., 2007). Furthermore, those simulations suggest that as the katabatic wind field increased in intensity it enhanced polar easterlies, and the expansion of sea-ice may have enhanced westerlies increasing ocean frontal divergence and upwelling, with possible implications for the marine carbon cycle and CO_2 drawdown observed in proxy records (Greenop et al., 2019; Masson-Delmotte et al., 2013; Pagani et al., 2011; Super et al., 2018; Zhang et al., 2013). Moreover, the long-term increase of 0.8‰ in carbon isotopes from 24 to 22.9 Ma (Fig. 8.2) has been attributed to an increase in global organic carbon burial and the associated reduction in atmospheric CO_2 (Mawbey and Lear, 2013; Paul et al., 2000; Stewart et al., 2017; Zachos et al., 1997).

Arguably even more remarkable than the Mi-1 glaciation, was its transient nature and the rapid deglaciation that followed within less than 100 kyrs (Greenop et al., 2019). The global ice volume loss may have been equivalent to as much as ~80 m of global sea-level rise implying continent-wide deglaciation of Antarctica according to some estimates (e.g. Miller et al., 2020) (Fig. 8.2), albeit the proxy sea-level estimates have significant uncertainties and are uncorrected for GIA. Atmospheric CO_2, reconstructed using the boron isotope method, appears to have rebounded by ~ 65ppm during the deglaciation from a low of ~265 ppm at the maximum of Mi-1 excursion, apparently in near-phase with a benthic $\delta^{18}O$ increase of +1.2‰ in the Atlantic Ocean equatorial ODP Site 926 record (Greenop et al., 2019) (Fig. 8.3), suggesting a direct coupling between the carbon cycle and orbitally-paced, ice-volume variability. This was in agreement with direct geological evidence for orbitally-driven fluctuations of the East Antarctic Ice Sheet (EAIS) from the dating of glacimarine sedimentary cycles in the Cape Roberts Project cores in the western Ross Sea (Naish et al., 2001). However, the magnitude of the implied OMT deglaciation is at odds with an oxygen-isotope enabled, ice-sheet

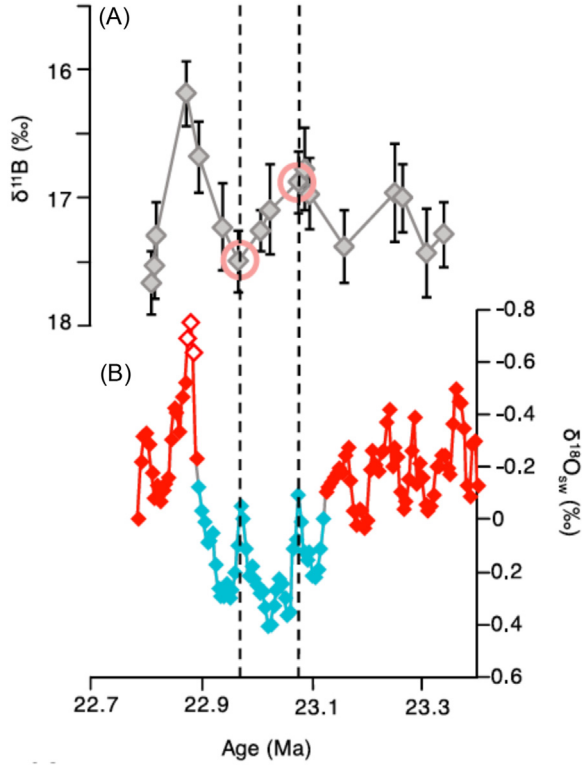

FIGURE 8.3 The relationship between $\delta^{11}B$ (Boron isotope atmospheric CO_2 proxy) and $\delta^{18}O_{sw}$ (global ice volume proxy) across the OMT. (A) The $\delta^{11}B$ record from Site 926 in the western equatorial Atlantic Ocean focused on 22.7–23.4 Ma from Greenop et al. (2019). The pink circles highlight $\delta^{11}B$ samples that fall within "peak glaciation conditions." Note the axis is reversed. (B) Relative $\delta^{18}O_{sw}$ change colour-coded for peak glacial (blue) and preglacial/postglacial conditions (red; Mawbey and Lear, 2013). Open circles are $\delta^{18}O_{sw}$ estimates within a dissolution event and therefore bias toward negative values. The dashed black lines show the coincident timing of the two $\delta^{11}B$ data points that sit on the pre/post-OMT/Mi-1 glaciation event lines.

modelling study by Gasson et al. (2016), that requires an extreme warm orbital configuration and atmospheric CO_2 concentration of more than 800 ppm to effect widespread retreat of terrestrial ice sheet. For a range of atmospheric CO_2 concentrations between 280 and 500 ppm, the $\delta^{18}O$ change was 0.52‰–0.66‰, or a sea level equivalent change of 30–36 m. Moreover, a recent transient ice sheet modelling study for deglaciations during the middle Miocene climatic optimum reveals significantly lower Antarctic ice volume variations (Stap et al., 2019), implying a relatively greater contribution by bottom water temperature to the $\delta^{18}O$ excursion. This modelling is consistent with a recent reconstruction of Middle-Late Miocene bottom water temperatures using Mg/Ca paleothermometry (Bradshaw et al., 2021). Intriguingly,

while Early Miocene CO_2 concentrations derived from marine proxies generally stay below ~500 ppm, two new quantitative CO_2 estimates using the stomatal leaf proxy method (Steinthorsdottir et al., 2019) and a leaf gas-exchange model (Reichgelt et al., 2016) from lake sediments in New Zealand suggest the CO_2 concentration may have been considerably higher, up to 1000 ppm (Steinthorsdottir et al., 2021). The well-dated, high-resolution varved record of the OMT from Foulden Maar implies atmospheric CO_2 more than doubled from ~500 ppm at the Mi-1 glacial maximum to ~1100 ppm within the first 20 kyr of the deglaciation phase (Reichgelt et al., 2016) (Fig. 8.2). While there are large uncertainties associated with the CO_2 proxy reconstructions, and the precise amplitude of the atmospheric CO_2 perturbation may be debatable, it appears to be orbitally-paced. Exactly how exchange between ocean and atmospheric reservoirs occurs at this magnitude and timescale remains an open question.

8.3.2 Apparent decoupling of Late Oligocene climate and ice volume?

Preceding the Mi-1 glaciation, a 3-Myr trend towards lower values (decrease up to ~1‰) in Late Oligocene (~27–24 Ma) composite benthic $\delta^{18}O$ records has been widely interpreted as a significant global warming event (e.g., Cramer et al., 2009; De Vleeschouwer et al., 2017; Liebrand et al., 2011, 2016, 2017; Westerhold et al., 2020; Zachos et al., 2001a) (Fig. 8.2). Bottom water temperature estimates using Mg/Ca paleothermometry on the same foraminiferal calcite as the $\delta^{18}O$ measurements suggest the mid-low latitude ocean warmed by up to 2°C (Billups and Schrag, 2002; Cramer et al., 2011). However, a $\delta^{18}O$ record from the high southern latitude Site ODP 690 on Maud Rise, displays a more muted decrease (Hauptvogel et al., 2017).

Paleoenvironmental information from stratigraphic drill cores in the Ross Sea region (Fig. 8.1) appears to preclude significant warming and, in fact, is more consistent with cooling during this time. Nannofossil, foraminiferal and marine macrofossil assemblages observed in DSDP Site 270 and CRP Ross Sea cores imply temperatures did not warm in regions proximal to the continent (Leckie and Webb, 1983; Taviani and Beu, 2003; Watkins and Villa, 2000). Moreover, pollen assemblages, clay minerals and chemical weathering indices in CRP cores record a cooling trend during the Late Oligocene (Ehrmann et al., 2005; Prebble et al., 2006a, 2006b; summarised in Barrett, 2007; Passchier and Krissek, 2008). In addition, orbitally-paced glacial advances recorded in shallow-marine sediments from western Ross Sea drill cores, showed the climate was periodically cold enough for EAIS trunk glaciers to down cut through the Transantarctic Mountains and ground on the inner continental shelf during the Late Oligocene (Hambrey et al., 1989; Naish et al., 2001; Roberts et al., 2003).

Late Oligocene glacio-eustatic sea-levels, reconstructed from sequence stratigraphic backstripping of shallow-marine continental margin records from sites in the far-field of the AIS, imply a long term lowering of global mean sea-level as ice grew on Antarctica from 26.5 Ma, with superimposed, orbital-scale sea-level fluctuations of up to $\pm \sim 50$ m (Miller et al., 2005, 2020; Kominz et al., 2008), although this magnitude of Antarctic ice volume variability remains difficult to reconcile in equilibrium or transient numerical ice sheet simulations (Gasson et al., 2016; Stap et al., 2019) (Figs 8.2, 8.4 and 8.5).

In contrast, cooling on the Wilkes Land margin of East Antarctica appears to have come later. A TEX_{86}-based sea-surface temperature (SST) record from IODP Site U1356 reveals a warming between 28–25 Ma followed by cooling through to ~23 Ma, culminating with the OMT (Hartman et al., 2018). A continuous Late Oligocene succession of contourites between 26 and 25 Ma at this site, records changes in bottom water strength and oxygenation interpreted to result from considerable fluctuations in oceanic

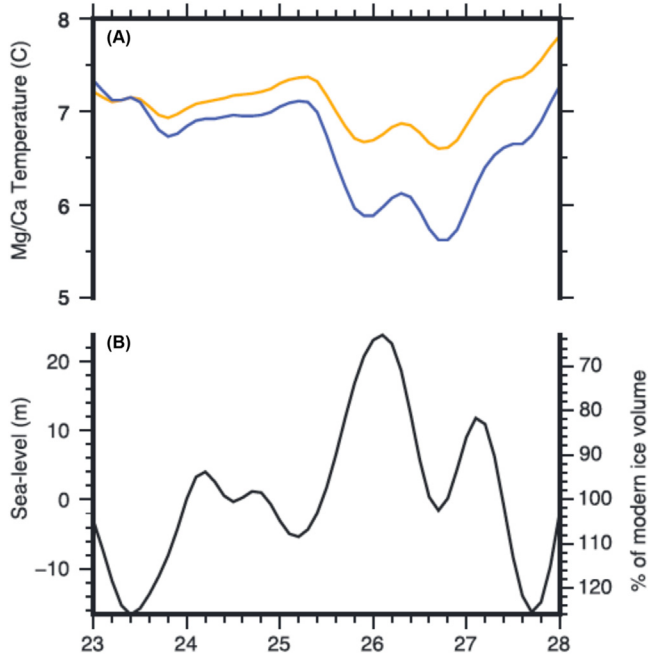

FIGURE 8.4 (A) Mg/Ca-based Pacific Ocean bottom water temperature estimates and (B) sea level with the per cent of modern ice volume estimates from Cramer et al. (2011) based on the sea level record of Kominz et al. (2008) and updated to the Gradstein et al. (2012) time scale. The blue line represents equation 7a and orange for equation 7b that Cramer et al. (2011) used to calculate bottom water temperature. Sea level is normalised to the modern ice volume equivalent of ~64 m. *Reproduced from Hauptvogel et al. (2017).*

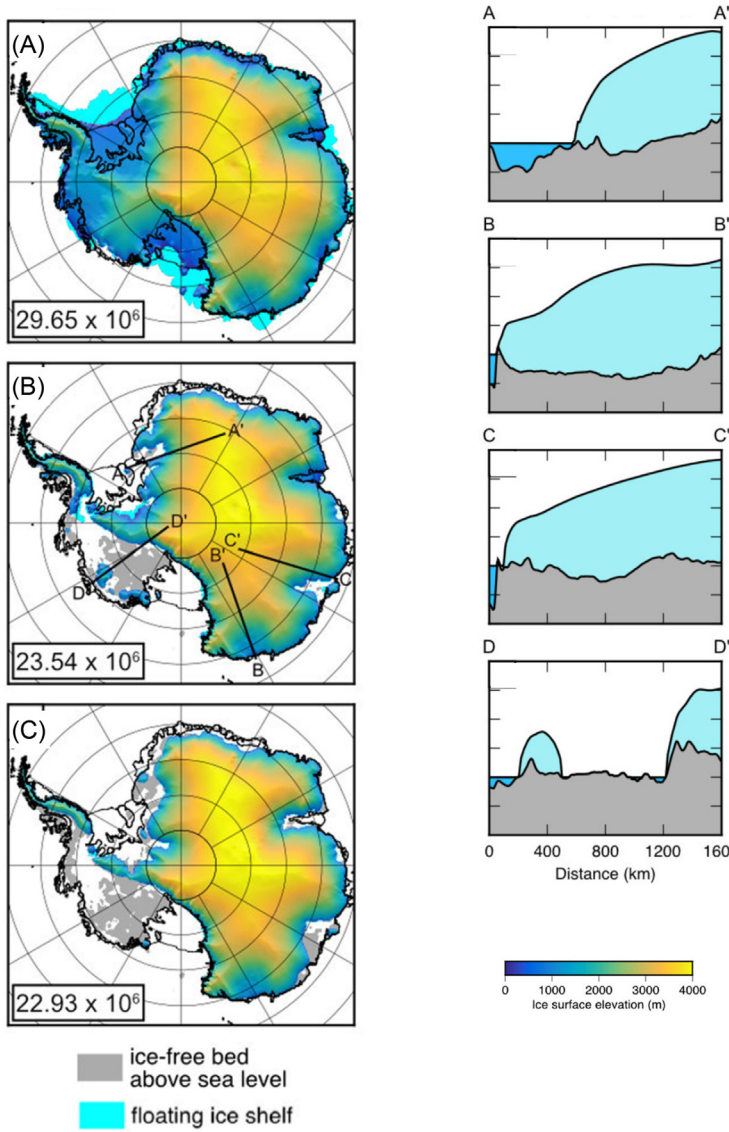

FIGURE 8.5 Ice sheet sensitivity to atmospheric CO_2 reconstructed and simulated for the Oligocene Miocene transition (OMT) after Paxman et al. (2020). (A) Shows an ice sheet grown under a colder climate ($pCO_2 = 280$ ppm) on the OMT median modern topography. (B) Shows the ice sheet elevation on the same topography following climate and ocean warming ($pCO_2 = 500$ ppm; 5°C ocean temperature rise). Profiles A-A′, B-B′, C-C′, and D-D′ are shown on the right. (C) Shows the ice sheet elevation following climate and ocean warming with a larger increase in pCO_2 to 840 ppm. Modelled total ice sheet volumes (in km^3) are given in each panel.

frontal systems in response to glacial-interglacial cycles paced by obliquity (Escutia et al., 2011; Salabarnada et al., 2018; Tauxe et al., 2012). Temperate surface waters between 27 and 25 Ma are also supported by the abundance of nannofossils preserved in the sediments (Escutia et al., 2011; Salabarnada et al., 2018), the lack of sea-ice-related dinocyst species and the relative abundance of oligotrophic, temperate dinocyst taxa (Bjil et al., 2018). Additionally, the absence of iceberg rafted debris (IRD) and reconstructions of cool-temperate vegetation (Strother et al., 2017) indicate that glaciers/ice caps were predominantly terrestrial occupying the topographic highs and lowlands in the now over-deepened Wilkes Subglacial Basin (Salabarnada et al., 2018). Cooling and development of marine-based ice on the Wilkes Land continental shelf occurred between ~25 and 23 Ma, and is expressed in Site U1356 cores as MTDs on the continental rise, associated with repeated AIS expansions to the shelf break during the latest Oligocene (Escutia et al., 2011; 2014; Evangelinos et al., 2020). However, episodic occurrence of carbonate cements, nannofossils and temperate dinocysts implies interglacials remained warm (e.g., Bjil et al., 2018; Escutia et al., 2011; Salabarnada et al., 2018), perhaps associated with orbitally-paced ocean front migration and CDW-upwelling (Evangelinos et al., 2020).

The disconnect between apparent cooling in some sectors of Antarctica and the warming implied by $\delta^{18}O$ records has been a source of ongoing investigation and speculation since a seminal paper by Barrett (2007) first pointed this out. One explanation invokes the development of poleward temperature gradient, whereby drill sites north of the Antarctic Circumpolar Current (ACC) were bathed with a warmer deep-water mass of Northern Hemisphere provenance (Pekar et al., 2006), while some sites south of the ACC were thermally-isolated (Scher et al., 2014), and under the influence of a locally produced cooler bottom waters (Hauptvogel et al., 2017). Furthermore, Hauptvogel et al. (2017) have argued that this may have masked AIS expansion in $\delta^{18}O$ records.

Notwithstanding this, the plot appears to thicken. While deep-water masses may explain the gradient in $\delta^{18}O$ between high and low latitudes, a trend towards lower $\delta^{18}O$ beginning after glacial Oi2b at 26.7 Ma and extending through the Late Oligocene (Fig. 8.2), is apparent in all benthic $\delta^{18}O$ records. Thus, unless temperature-dependent fractionation of foraminiferal calcite dominates the overall $\delta^{18}O$ signature during this time (i.e., the opposite of Quaternary $\delta^{18}O$ records), then AIS volume must have decreased despite the far-field sea-level records implying a global mean sea-level fall.

Continental-scale ice sheet models using restored Antarctic paleogeography for time slices in the Oligocene and Miocene (e.g., Paxman et al., 2019; Wilson and Luyendyk, 2009) are able to store more ice on west Antarctica than today (Colleoni et al., 2018, 2021; Gasson et al., 2016; Paxman et al., 2020; Wilson et al., 2002, 2013). This is because much of the region was

subaerial providing more land area for a large terrestrial ice sheet to develop (De Santis et al., 1995, 1999; Paxman et al., 2019; Wilson and Luyendyk, 2009), Based on evidence from seismic data (De Santis et al., 1995), and sediments in the central Ross Sea from DSDP Site 270 (e.g. Kulhanek et al., 2019, Leckie and Webb, 1983) (Fig. 8.2), a number of authors have proposed that a marine transgression across West Antarctica began at ~26 Ma when it tectonically-subsided, and this may have caused ocean-induced melt of a significant part of the terrestrial West Antarctica Ice Sheet (WAIS) (Greenop et al., 2019; Levy et al., 2016; Liebrand et al., 2017). This resulted in a gradual and progressive decrease in AIS extent and volume through the Late Oligocene, and may account for the overall decrease in average $\delta^{18}O$ values in the benthic isotope stacks (e.g., Cramer et al.; 2009; De Vleeschouwer et al., 2017; Zachos et al., 2001a).

While this potentially provides a tantalising explanation for the apparent decoupling between atmospheric CO_2 and ice volume, as expressed in the benthic $\delta^{18}O$ record during the Late Oligocene, the evidence for circum-Antarctic surface ocean cooling is ambiguous. More high-quality sea-surface temperature and climate records will be needed to confirm this hypothesis.

A further wrinkle in this reconciliation of global and Antarctic Late Oligocene climate and ice volume proxy records, is the apparent fall in global sea-level between ~26 and 23 Ma implied by far-field sea-level records from the New Jersey continental margin (Hauptvogel et al., 2017; Kominz et al., 2008; Miller et al., 2020; Fig. 8.4). We suggest, that ongoing efforts should focus on improving the precision of the age models and reducing uncertainties for far-field continental margin sea-level estimates and their correlation with benthic $\delta^{18}O$ records.

8.4 Concluding remarks

Considerable progress has been made over the last 10 years in our understanding of AIS dynamics across the OMT from analysis of both geological records and the improvement of numerical ice sheet models. When the first edition of this chapter was written (Wilson et al., 2009), numerical ice sheet models displayed strong hysteresis due to surface elevation−mass balance feedback as a result of the atmospheric lapse rate and surface albedo, possibly strengthened by the cooling effect of the ice sheet on the surrounding Southern Ocean (DeConto et al., 2007; Ladant et al., 2014; Pollard and DeConto 2005). Since then, four developments by the modelling community have resulted in a much better comparison between models and data: (1) A climate−ice sheet coupling method that uses a high-resolution atmospheric model to account for ice sheet−climate feedbacks (e.g., Gasson et al., 2016); (2) The ability to model instability mechanisms that act only on marine-based ice, particularly where the ice sits on reverse-sloped beds (e.g., Pollard and DeConto, 2009); (3) Some ice sheet models now include mechanisms for retreat into deep subglacial basins caused by ice-cliff failure and ice-shelf hydrofracture (e.g., DeConto and

Pollard, 2016; Pollard et al., 2015); and (4) Models now have the ability to account for changes in the oxygen isotopic composition of the ice sheet by using isotope-enabled climate and ice sheet models (Gasson et al., 2016).

Notwithstanding this progress, challenges still remain in model development and parameterisation, the quality, precision, and stratigraphic completeness of proxy data and our ability to develop high-resolution chronologies for Antarctic margin and Southern Ocean records, as outlined in the Introduction section (see also Siegert and Golledge, 2021). To address this, more ice-proximal to ice-distal marine sediment cores are needed to understand and reconcile regional differences (e.g., Wilkes Land vs Ross Sea), which result from differing tectonic subsidence histories and sub-glacial basin topographies affecting ice drainage and ocean-ice connections.

In this chapter we have summarised the latest proxy datasets for ice volume, atmospheric CO_2, ocean carbon cycle dynamics and ocean temperature, to build a data-driven picture of a highly dynamic AIS across the OMT. The AIS initially evolved from a terrestrial ice sheet into a marine-based ice sheet for the first time, which was perhaps 120% larger than today, and then retreated with ice potentially disappearing from the Antarctic continental interior implying a very rapid, Late Quaternary Northern Hemisphere-style, orbitally-modulated, CO_2-driven continental-scale collapse and deglaciation.

The OMT provides insights into the potential of threshold behaviour, irreversible on human timescales, if certain CO_2 concentrations are crossed (e.g., 400 ppm) (e.g. Masson-Delmotte et al., 2013). In this chapter, we have highlighted the relative roles of CO_2 and orbital forcing, agreeing with model predictions (e.g., DeConto et al., 2008; Gasson et al., 2016; Pollard and DeConto, 2009) and strengthening geological evidence (e.g., Escutia et al., 2011, 2014; Levy et al., 2016, 2019; Naish et al., 2009) that the AIS is highly dynamic within a relatively small range of atmospheric CO_2 concentrations. Proxy data and model simulations suggest thresholds for glaciation (e.g. LGM, see Siegert et al., 2021) and loss of marine-based ice sheets may be around 300 and 400 ppm, respectively (e.g., DeConto et al., 2008; Foster and Rohling, 2013; Levy et al., 2019). Under sustained current atmospheric CO_2 levels of 400 ppm, the Intergovernmental Panel on Climate Change 5th Assessment Report (Masson-Delmotte et al., 2013), states orbital forcing alone cannot cause a future LGM-style glaciation. This report also implies that we may be close to initiating irreversible loss of Antarctica's marine based ice sheets, potentially taking our world back to the Pliocene when sea-levels were ~20 m higher than today (e.g., Grant and Naish, 2021; Grant et al., 2019).

Acknowledgements

T.N., B.D., R.L., and R.M. were funded by the NZ MBIE Antarctic Science Platform (ANTA1801). R.M. was also funded by the Royal Society of New Zealand Te Apārangi Marsden Fund (18-VUW-089). L.D.S. and F.D. were funded by the Programma Nazionale delle Ricerche in Antartide (PNRA16_00016 project and PNRA 14_00119). C.E.

acknowledges funding by the Spanish Ministry of Science and Innovation (grant CTM2017-89711-C2-1/2-P), co-funded by the European Union through FEDER funds.

References

Badger, M., Lear, C.H., Pancost, R.D., Foster, G.L., Bailey, T., et al., 2013. CO_2 drawdown following the middle Miocene expansion of the Antarctic Ice Sheet. Paleoceanography 28, 42–53. Available from: https://doi.org/10.1002/palo.20015.

Barker, P.F., Carmerlenghi, A., Acton, G.D., et al., 1999. Proceedings of the Ocean Drilling Program, Initial reports, v. 178. Ocean Drilling Program, College Station, TX [online].

Barker, P.F., Kennett, J.P.Scientific Party, 1988. Weddell Sea Palaeoceanography: preliminary results of ODP Leg 113. Palaeogeography, Palaeoclimatology, Palaeoecology 67, 75–102.

Barrett, P.J., 2007. Cenozoic climate and sea level history from glacimarine strata off the Victoria Land coast, Cape Roberts Project, Antarctica. In: Hambrey, M.J., Christoffersen, P., Glasser, N.F., Hubbard, B. (Eds.), Glacial Sedimentary Processes and Products, 39. International Association of Sedimentologists, pp. 259–287.

Barron, J., Larsen, B., et al., 1989. College Station, TX (Ocean Drilling Program). doi:10.2973/odp.proc.ir.119.1989. Proc. ODP, Init. Repts. 119. Available from: https://doi.org/10.2973/odp.proc.ir.119.1989.

Bartoli, G., Hönisch, B., Zeebe, R.E., 2011. Atmospheric CO_2 decline during the Pliocene intensification of Northern Hemisphere glaciations. Paleoceanography 26 (4). Available from: https://doi.org/10.1029/2010PA002055.

Berggren, W.A., Kent, D.V., Flynn, J., Van Couvering, J.A., 1985. Cenozoic geochronology. Geological Society of America Bulletin 96, 1407–1418.

Bijl, P.K., Bendle, J.A., Bohaty, S.M., Pross, J., Schouten, S., Tauxe, L., et al.,Expedition 318 Scientists 2013. Eocene cooling linked to early flow across the Tasmanian Gateway. Proceedings of the National Academy of Sciences of the United States of America 110 (24), 9645–9650. Available from: https://doi.org/10.1073/pnas.1220872110.

Billups, K., Pälike, H., Channell, J.E.T., Zachos, J.C., Shackleton, N.J., 2004. Astronomic calibration of the late Oligocene through early Miocene geomagnetic polarity time scale. Earth and Planetary Science Letters 224, 33–44.

Billups, K., Schrag, D.P., 2002. Paleotemperatures and ice volume of the past 27 Myr revisited with paired Mg/Ca and $^{18}O/^{16}O$ measurements on benthic foraminifera. Paleoceanography 17. Available from: https://doi.org/10.1029/2000PA000567.

Bjil, P.K., Houben, A.J.P., Hartman, J.D., Pross, J., Salabarnada, A., Escutia, C., et al., 2018. Paleoceanography and ice sheet variability off-shore Wilkes Land, Antarctica – Part 2: Insights from Oligocene–Miocene dinoflagellate cyst assemblages. Climate of the Past 14, 1015–1033. Available from: https://doi.org/10.5194/cp-14-1015-2018.

Bradshaw, C.D., Langebroek, P.M., Lear, C.H., et al., 2021. Hydrological impact of Middle Miocene Antarctic ice-free areas coupled to deep ocean temperatures. Nature Geoscience. Available from: https://doi.org/10.1038/s41561-021-00745-w.

Cande, S.C., Kent, D.V., 1992. A new geomagnetic polarity timescale for the Late Cretaceous and Cenozoic. Journal of Geophysical Research 97, 13917–13951.

Cande, S.C., Kent, D.V., 1995. Revised calibration of the geomagnetic polarity timescale for the Late Cretaceous and Cenozoic. Journal of Geophysical Research 100, 6093–6095.

Colleoni, F., De Santis, L., Montoli, E., Olivo, E., Sorlien, C.C., Bart, P.J., et al., 2018. Past continental shelf evolution increased Antarctic ice sheet sensitivity to climatic conditions. Scientific Reports 8, 11323. Available from: https://doi.org/10.1038/s41598-018-29718-7.

Colleoni, F., et al., PAIS community 2021. Past Antarctic ice sheet dynamics (PAIS) and implications for future sea-level change. In: Florindo, F., et al., (Eds.), Antarctic Climate Evolution, Second ed. Elsevier.

Cooper, A.K., O'Brien, P.E., 2004. Leg 188 synthesis: transitions in the glacial history of the Prydz Bay Region, East Antarctica, from ODP Drilling. Proceedings of the Ocean Drilling Programme, Scientific Results 188. Available from: https://doi.org/10.2973/odp.proc.sr.188.001.2004.

Coxall, H.K., Wilson, P.A., Pälike, H., Lear, C.H., Backman, J., 2005. Rapid stepwise onset of Antarctic glaciation and deeper calcite compensation in the Pacific Ocean. Nature 433 (7021), 53–57.

Cramer, B.S., Miller, K.G., Barrett, P.J., Wright, J.D., 2011. Late Cretaceous–Neogene trends in deep ocean temperature and continental ice volume: Reconciling records of benthic foraminiferal geochemistry ($\delta^{18}O$ and Mg/Ca) with sea level history. Journal of Geophysical Research 116, C12023. Available from: https://doi.org/10.1029/2011JC007255.

Cramer, B.S., Toggweiler, J.R., Wright, J.D., Katz, M.E., Miller, K.G., 2009. Ocean overturning since the Late Cretaceous: inferences from a new benthic foraminiferal isotope compilation. Paleoceanography 24, PA4216. Available from: https://doi.org/10.1029/2008PA001683.

Crampton, J.S., Cody, R.D., Levy, R., Harwood, D., McKay, R., Naish, T.R., 2016. Southern Ocean phytoplankton turnover in response to stepwise Antarctic cooling over the past 15 million years. Proceedings of the National Academy of Sciences 113 (25), 6868–6873.

De Santis, L., Anderson, J.B., Brancolini, G., Zayatz, I., 1995. In: Cooper, A.K., et al., (Eds.), Antarctic Research Series, vol. 71. Springer International, pp. 235–260.

De Vleeschouwer, D., Vahlenkamp, M., Crucifix, M., Pälike, H., 2017. Alternating Southern and Northern Hemisphere climate response to astronomical forcing during the past 35 m.y. Geology 45 (4), 375–378. Available from: https://doi.org/10.1130/G38663.1.

DeConto, R., Pollard, D., Wilson, P., et al., 2008. Thresholds for Cenozoic bipolar glaciation. Nature 455, 652–656. Available from: https://doi.org/10.1038/nature07337.

DeConto, R.M., Pollard, D., 2016. Contribution of Antarctica to past and future sea level rise. Nature 531, 591–597. Available from: https://doi.org/10.1038/nature17145.

DeConto, R.M., Pollard, D., Harwood, D., 2007. Sea ice feedback and Cenozoic evolution of Antarctic climate and ice sheets. Paleoceanography 22, PA3214. Available from: https://doi.org/10.1029/2006PA001350.

Donda, F., O'Brien, P.E., De Santis, L., Rebesco, M., Brancolini, G., 2008. Mass wasting processes in the Western Wilkes Land margin: Possible implications for East Antarctic glacial history. Palaeogeography, Palaeoclimatology, Palaeoecology 260, 77–91.

Ehrmann, W., Setti, M., Marinoni, L., 2005. Clay minerals in Cenozoic sediments off Cape Roberts (McMurdo Sound, Antarctica) reveal palaeoclimatic history. Palaeogeography, Palaeoclimatology, Palaeoecology 229, 187–211.

Escutia, C., De Santis, L., Donda, F., Dunbar, R.B., Brancolini, G., Eittreim, S.L., et al., 2005. Cenozoic ice sheet history from east Antarctic Wilkes Land continental margin sediments. Global and Planetary Change 45 (1–3), 51–81.

Escutia, C., Brinkhuis, H.and the Expedition 318 Science Party, 2014. From greenhouse to icehouse at the Wilkes Land Antarctic margin: IODP 318 synthesis of results. Developments in Marine Geology 7, 295–328. Available from: https://doi.org/10.1016/B978-0-444-62617-2.00012-8.

Escutia, C., Brinkhuis, H., Klaus, A., and the Expedition 318 Scientists, 2011. Proceedings of the IODP, vol. 318, Tokyo (Integrated Ocean Drilling Program Management International, Inc.). doi:10.2204/iodp.proc.318.2011.

Escutia, C., Eittreim, S., Cooper, A.K., 1997. Cenozoic sedimentation on the Wilkes Land continental rise, Antarctica. In: Ricci, C.A. (Ed.), The Antarctic Region: Geological Evolution and Processes. Terra Antartica, pp. 791–795.

Evangelinos, D., Escutia, C., Etourneau, J., Hoem, F., Bijl, P., Boterblom, W., et al., 2020. A. Late Oligocene-Miocene proto-Antarctic circum polar current dynamics off the Wilkes Land margin, east Antarctica. Global and Planetary Change 191, 103221. Available from: https://doi.org/10.1016/j.gloplacha.2020.103221.

Foster, G.L., Lear, C.H., Rae, J., W., B., 2012. The evolution of pCO_2, ice volume and climate during the middle Miocene. Earth and Planetary Science Letters 341–344, 243–254. Available from: https://doi.org/10.1016/j.epsl.2012.06.007.

Foster, G., Rohling, E., 2013. Relationship between sea level and climate forcing by CO_2 on geological timescales. PNAS. 110. Available from: https://doi.org/10.1073/pnas.1216073110.

Fraass, A., Leckie, M., DeConto, R., McQuaid, C., Burns, S., Zachos, J., 2019. Reappraisal of Oligocene–Miocene chronostratigraphy and the Mi-1 event: ocean drilling program site 744, Kerguelen Plateau, southern Indian Ocean. Stratigraphy 15 (4), 265–278.

Galeotti, S., DeConto, R.M., Naish, T.R., Stocchi, P., Florindo, F., Pagani, M., et al., 2016. Antarctic ice sheet variability across the Eocene–Oligocene boundary climate transition. Science 352, 76–80. Available from: https://doi.org/10.1126/science.aab0669.

Gasson, E., DeConto, R.M., Pollard, D., Levy, R., 2016. Dynamic Antarctic ice sheet during the early to mid-Miocene. Proceedings of the National Academy of Sciences of the United States of America 113 (13), 3,459–3,464. Available from: https://doi.org/10.1073/pnas.1516130113.

Gradstein, F.M., Ogg, J.G., Smith, A.G. (Eds.), 2004. A Geological Time Scale. Cambridge University Press, Cambridge, p. 589.

Gradstein, F.M., Ogg, J.G., Schmitz, M.D., Ogg, G.M., 2012. The geological time scale 2012. Elsevier B.V., Oxford, U.K.

Grant, G.R., Naish, T.R., Dunbar, G.B., Stocchi, P., Kominz, M.A., Kamp, P.J., et al., 2019. The amplitude and origin of sea-level variability during the Pliocene epoch. Nature 574 (7777), 237–241. Available from: https://doi.org/10.1038/s41586-019-1619-z. doi.org/10.22498/pages.29.1.4.

Grant, G., Naish, T., 2021. Pliocene sea-level revisited: is there more than meets the eye? PAGES Magazine 29, doi.org/10.22498/pages.29.1.4.

Greenop, R., Foster, G.L., Wilson, P.A., Lear, C.H., 2014. Middle Miocene climate instability associated with high-amplitude CO_2 variability. Paleoceanography 29. Available from: https://doi.org/10.1002/2014PA002653.

Greenop, R., Sosdian, S.M., Henehan, M.J., Wilson, P.A., Lear, C.H., Foster, G.L., 2019. Orbital forcing, ice volume, and CO_2 Across the Oligocene-Miocene Transition. Paleoceanography and Paleoclimatology 34 (3), 316–328. Available from: https://doi.org/10.1029/2018PA003420.

Gulick, S., Shevenell, A., Montelli, A., et al., 2017. Initiation and long-term instability of the East Antarctic Ice Sheet. Nature 552, 225–229. Available from: https://doi.org/10.1038/nature25026.

Hambrey, M.J., Barrett, P.J., Robinson, P.H., 1989. Stratigraphy. In Barrett, P.J. (Ed.), Antarctic Cenozoic History from the CIROS-1 Drillhole, McMurdo Sound. DSIR Publishing, Wellington, New Zealand, pp. 23–48.

Hambrey, M.J., Ehrmann, W.U., Larsen, B., 1991. Cenozoic glacial record of the Prydz Bay Continental Shelf, East Antarctica. Proceedings of the Ocean Drilling Programme, Scientific Results 120, 77–132.

Hartman, J.D., Sangiorgi, F., Salabarnada, A., Peterse, F., Houben, A.J., Schouten, S., et al., 2018. Paleoceanography and ice sheet variability offshore Wilkes Land, Antarctica-Part 3: insights from Oligocene-Miocene TEX86-based sea surface temperature reconstructions. Climate of the Past 14 (9), 1275–1297. Available from: https://doi.org/10.5194/cp-14-1275-2018.

Hauptvogel, D.W., Pekar, S.F., Pincay, V., 2017. Evidence for a heavily glaciated Antarctica during the late Oligocene "warming" (27.8–24.5 Ma): Stable isotope records from ODP Site 690. Paleoceanography 32 (4), 384–396.

Hochmuth, K., Gohl, K., Leitchenkov, G., Sauermilch, I., Whittaker, J.M., Uenzelmann-Neben, G., et al., 2020. The evolving paleobathymetry of the circum-Antarctic Southern Ocean since 34 Ma – a key to understanding past cryosphere-ocean developments. Geochemistry, Geophysics, Geosystems e2020GC009122. Available from: https://doi.org/10.1029/2020GC009122.

Honisch, B., Hemming, G., Archer, D., Siddal, M., McManus, J., 2009. Atmospheric carbon dioxide concentration across the Mid-Pleistocene Transition. Science 324, 1551–1554. Available from: https://doi.org/10.1126/science.1171477.

Kennett, J.P., 1977. Cenozoic evolution of Antarctic glaciation, the circum-Antarctic Ocean, and their impact on global paleoceanography. Journal of Geophysical Research 82, 3843–3860.

Kennett, J.P., Houtz, R.E., et al., 1974. Initial Reports of the Deep Sea Drilling Project, vol. 29. U.S. Government Printing Office, Washington, DC, p. 1197.

Kominz, M.A., Browning, J.V., Miller, K.G., Sugarman, P.J., Mizintseva, S., Scotese, C.R., 2008. Late cretaceous to Miocene sea-level estimates from the New Jersey and Delaware coastal plain coreholes: an error analysis. Basin Research 20 (2), 211–226. Available from: https://doi.org/10.1111/j.1365-2117.2008.00354.x.

Kulhanek, D.K., Levy, R.H., Clowes, C.D., Prebble, J.G., Rodelli, D., Jovane, L., et al., 2019. Revised chronostratigraphy of DSDP Site 270 and late Oligocene to early Miocene paleoecology of the Ross Sea sector of Antarctica. Global and Planetary Change 178, 46–64.

Ladant, J.B., Donnadieu, Y., Lefebvre, V., Dumas, C., 2014. The respective role of atmospheric carbon dioxide and orbital parameters on ice sheet evolution at the Eocene–Oligocene transition. Paleoceanography 29 (8), 810–823.

Laskar, J., Robutel, P., Joutel, F., Gastineau, M., Correia, A.C.M., Levrard, B., 2004. A long-term numerical solution for the insolation quantities of the Earth. Astronomy and Astrophysics 428 (1), 261–285. Available from: https://doi.org/10.1051/0004-6361:20041335.

Lear, C.H., Coxall, H.K., Foster, G.L., Lunt, D.J., Mawbey, E.M., Rosenthal, Y., et al., 2015. Neogene ice volume and ocean temperatures: Insights from infaunal foraminiferal Mg/Ca paleothermometry. Paleoceanography 30, 1437–1454. Available from: https://doi.org/10.1002/2015PA002833.

Leckie, R.M., Webb, P.-N., 1983. Late Oligocene–early Miocene glacial record of the Ross Sea, Antarctica: evidence from DSDP Site 270. Geology 11, 578–582.

Levy, R., Harwood, D., Florindo, F., Sangiorgi, F., Tripati, R., von Eynatten, H., et al., 2016. SMS science team. 2016. Early to mid-Miocene Antarctic ice sheet dynamics. Proceedings of the National Academy of Sciences 113 (13), 3453–3458. Available from: https://doi.org/10.1073/pnas.1516030113.

Levy, R.H., Meyers, S.R., Naish, T.R., Golledge, N.R., McKay, R.M., Crampton, J.S., et al., 2019. Antarctic ice-sheet sensitivity to obliquity forcing enhanced through ocean connections. Nature Geoscience 12, 132–137. Available from: https://doi.org/10.1038/s41561-018-0284-4.

Liebrand, D., Beddow, H.M., Lourens, L.J., et al., 2016. Cyclostratigraphy and eccentricity tuning of the early Oligocene through early Miocene (30.1–17.1 Ma): cibicides mundulus stable oxygen and carbon isotope records from Walvis Ridge Site 1264. Earth and Planetary Science Letters 450, 392–405.

Liebrand, D., de Bakker, A., Beddow, H., Wilson, P., Bohaty, S., Ruessink, G., et al., 2017. Evolution of the early Antarctic ice ages. Proceedings of the National Academy of Sciences 114 (15), 3867–3872. Available from: https://doi.org/10.1073/pnas.1615440114.

Liebrand, D., Lourens, L.J., Hodell, D.A., de Boer, B., van de Wal, R.S.W., Palike, H., 2011. Antarctic ice sheet and oceanographic response to eccentricity forcing during the early Miocene. Climate of the Past 7 (3), 869–880. Available from: https://doi.org/10.5194/cp-7-869-2011.

Martinez-Boti, M.A., Foster, G.L., Chalk, T.B., Rohling, E.J., Sexton, P.F., et al., 2015. Plio-Pleistocene climate sensitivity evaluated using high-resolution CO_2 records. Nature 518, 49–54. Available from: https://doi.org/10.1038/nature14145.

Masson-Delmotte, V., Schulz, M., Abe-Ouchi, A., Beer, J., Ganopolski, A., Gonzáles Rouco, J.F., et al., 2013. Information from paleoclimate archives. In: Stocker, T.F., Qin, D., Plattner, G.K., Tignor, M., Allen, S.K., Boschung, J., et al.,Climate Change 2013: The Physical Science Basis. Contribution of Working Group I to the Fifth Assessment Report of the Intergovernmental Panel on Climate Change. Cambridge University Press, Cambridge, UK and New York.

Mawbey, E.M., Lear, C.H., 2013. Carbon cycle feedbacks during the Oligocene–Miocene transient glaciation. Geology 41 (9), 963–966. Available from: https://doi.org/10.1130/G34422.1.

McKay, R., et al., 2021. Cenozoic History of Antarctic Glaciation and Climate from Onshore and Offshore Studies. In: Florindo, F., et al., (Eds.), Antarctic Climate Evolution, Second ed. Elsevier.

Miller, K.G., Browning, J.V., Schmelz, W.J., Kopp, R.E., Mountain, G.S., Wright, J.D., 2020. Cenozoic sea-level and cryospheric evolution from deep-sea geochemical and continental margin records. Science Advances 6 (20), eaaz1346. Available from: https://doi.org/10.1126/sciadv.aaz1346.

Miller, K.G., Kominz, M.A., Browning, J.V., Wright, J.D., Mountain, G.S., Katz, M.E., et al., 2005. The phanerozoic record of global sea-level change. Science 310 (5752), 1293–1298. Available from: https://doi.org/10.1126/science.1116412.

Miller, K.G., Wright, J.D., Fairbanks, R.G., 1991. Unlocking the ice house: Oligocene–Miocene oxygen isotopes, eustasy, and margin erosion. Journal of Geophysical Research: Solid Earth 96 (B4), 6829–6848. Available from: https://doi.org/10.1029/90JB02015.

Naish, T., Powell, R., Levy, R., Wilson, G., Scherer, R., Talarico, F., et al., 2009. Obliquity-paced Pliocene West Antarctic ice sheet oscillations. Nature 458, 322–328. Available from: https://doi.org/10.1038/nature07867.

Naish, T.R., Wilson, G.S., Dunbar, G., Barrett, P.J., 2008. Constraining the amplitude of late Oligocene bathymetric changes in western Ross Sea during orbitally-induced oscillations in the East Antarctic ice sheet: (2) Implications for global sea–level changes. Palaeogeography, Palaeoclimatology, Palaeoecology 260, 55–65.

Naish, T.R., Woolfe, K.J., Barrett, P.J., Wilson, G.S., Atkins, C., Bohaty, S., et al., 2001. Orbitally induced oscillations in the East Antarctic ice sheet at the Oligocene/Miocene boundary. Nature 413, 719–723.

Pagani, M., Liu, Z., LaRiviere, J., Ravelo, A.C., 2010. High Earth-system climate sensitivity determined from Pliocene carbon dioxide concentrations. Nature Geoscience 3, 27–30. Available from: https://doi.org/10.1038/ngeo724.

Pagani, M., Zachos, J.C., Freeman, K.H., Tipple, B., Bohaty, S., 2005. Carbon dioxide concentrations during the Paleogene. Science 309, 600–603. Available from: https://doi.org/10.1126/science.1110063.

Pagani, M., Huber, M., Liu, Z., Bohaty, S., Henderiks, J., et al., 2011. The role of carbon dioxide during the onset of Antarctic glaciation. Science 334, 1261–1264. Available from: https://doi.org/10.1126/science.1203909.

Pälike, H., Laskar, J., Shackleton, N.J., 2004. Geologic constraints on the chaotic diffusion of the solar system. Geology 32, 929–932.

Pälike, H., Norris, R.D., Herrle, J.O., Wilson, P.A., Coxall, H.K., Lear, C.H., et al., 2006. The heartbeat of the Oligocene climate system. Science 314, 1894–1898.

Passchier, S., Krissek, L.A., 2008. Oligocene-Miocene Antarctic continental weathering record and paleoclimatic implications, Cape Roberts Drilling Project, Ross Sea, Antarctica. Palaeogeography, Palaeoclimatology, Palaeoecology 260, 30–40.

Paul, H., Zachos, J.C., Flower, B., Tripati, A., 2000. Orbitally induced climate and geochemical variability across the Oligocene/Miocene boundary. Paleoceanography 15 (5), 471–485. Available from: https://doi.org/10.1029/1999PA000443.

Paxman, G.J.G., Gasson, E.G.W., Jamieson, S.S.R., Bentley, M.J., Ferraccioli, F., 2020. Long-term increase in Antarctic ice sheet vulnerability driven by bed topography evolution. Geophysical Research Letters 47, e2020GL090003. Available from: https://doi.org/10.1029/2020GL090003.

Paxman, G.J., Jamieson, S.S., Hochmuth, K., Gohl, K., Bentley, M.J., Leitchenkov, G., et al., 2019. Reconstructions of Antarctic topography since the Eocene–Oligocene boundary. Palaeogeography, Palaeoclimatology, Palaeoecology 535, 109346. Available from: https://doi.org/10.1016/j.palaeo.2019.109346.

Pekar, S.F., DeConto, R.M., Harwood, D.M., 2006. Resolving a late Oligocene conundrum: deep-sea warming and Antarctic glaciation. Palaeogeography, Palaeoclimatology, Palaeoecology 231 (1–2), 29–40.

Pekar, S.F., Christie-Blick, N., Kominz, M.A., Miller, K.G., 2002. Calibration between eustatic estimates from backstripping and oxygen isotopic records for the Oligocene. Geology 30 (10), 903–906. Available from: https://doi.org/10.1130/0091-7613.

Pekar, S.F., Kominz, M.A., 2001. Two-dimensional paleoslope modeling: a new methods for estimating water depths for benthic foraminiferal biofacies and paleo shelf margins. Journal of Sedimentary Research 71, 608–620.

Pollard, D., DeConto, R.M., 2005. Hysteresis in Cenozoic Antarctic ice-sheet variations. Global and Planetary Change 45 (1–3), 9–21. Available from: https://doi.org/10.1016/j.gloplacha.2004.09.011.

Pollard, D., DeConto, R.M., 2009. Modelling West Antarctic ice sheet growth and collapse through the past five million years. Nature 458 (7236), 329–332. Available from: https://doi.org/10.1038/nature07809.

Pollard, D., DeConto, R.M., Alley, R.B., 2015. Potential Antarctic ice sheet retreat driven by hydrofracturing and ice cliff failure. Earth and Planetary Science Letters 412, 112–121. Available from: https://doi.org/10.1016/j.epsl.2014.12.035.

Prebble, J.G., Hannah, M.J., Barrett, P.J., 2006a. Changing Oligocene climate recorded by palynomorphs from two glacio-eustatic sedimentary cycles, Cape Roberts Project, Victoria Land Basin, Antarctica. Palaeogeography, Palaeoclimatology, Palaeoecology 231 (1–2), 58–70.

Prebble, J.G., Raine, J.I., Barrett, P.J., Hannah, M.J., 2006b. Vegetation and climate from two Oligocene glacioeustatic sedimentary cycles (31 and 24 Ma) cored by the Cape Roberts Project, Victoria Land Basin, Antarctica. Palaeogeography, Palaeoclimatology, Palaeoecology 231 (1–2), 41–57.

Raymo, M.E., Kozdon, R., Evans, D., Lisiecki, L., Ford, H., 2018. The accuracy of mid-Pliocene $\delta^{18}O$-based ice volume and sea level reconstructions. Earth-Science Reviews 177, 291–302. Available from: https://doi.org/10.1016/j.earscirev.2017.11.022.

Reichgelt, T., D'Andrea, W.J., Fox, B.R., 2016. Abrupt plant physiological changes in southern New Zealand at the termination of the Mi-1 event reflect shifts in hydroclimate and pCO_2. Earth and Planetary Science Letters 455, 115–124.

Roberts, A.P., Wilson, G.S., Harwood, D.M., Verosub, K.L., 2003. Glaciation across the Oligocene-Miocene boundary in southern McMurdo Sound, Antarctica: new chronology from the CIROS-1 drill hole. Palaeogeography, Palaeoclimatology, Palaeoecology 198, 113–130.

Salabarnada, A., Escutia, C., Röhl, U., Nelson, C.H., McKay, R., Jiménez-Espejo, F.J., et al., 2018. Paleoceanography and ice sheet variability offshore Wilkes Land, Antarctica – part 1: insights from late Oligocene astronomically paced contourite sedimentation. Climates of the Past 14, 991–1014. Available from: https://doi.org/10.5194/cp-14-991-2018.

Sangiorgi, F., Bijl, P.K., Passchier, S., Salzmann, U., Schouten, S., McKay, R., et al., 2018. Southern Ocean warming and Wilkes Land ice sheet retreat during the mid-Miocene. Nature Communications 9 (1), 1–11. Available from: https://doi.org/10.1038/s41467-017-02609-7.

Scher, H.D., Bohaty, S.M., Smith, B.W., Munn, G.H., 2014. Isotopic interrogation of a suspected late Eocene glaciation. Paleoceanography 29 (6), 628–644.

Schlich, R., Wise Jr, S.W., 1992. The geologic and tectonic evolution of the Kerguelen Plateau: an introduction to the scientific results of Leg 120. Proceedings of the Ocean Drilling Programme, Scientific results 120, 5–30.

Seki, O., Foster, G.L., Schmidt, D.N., Mackensen, A., Kawamura, K., Pancost, R.D., 2010. Alkenone and boron based Plio-Pleistocene pCO_2 records. Earth and Planetary Science Letters 292, 201–211. Available from: https://doi.org/10.1016/j.epsl.2010.01.037.

Shackleton, N.J., Hall, M.A., Raffi, I., Tauxe, L., Zachos, J., 2000. Astronomical calibration for the Oligocene–Miocene boundary. Geology 28, 447–450.

Shevenell, A.E., Kennett, J.P., Lea, D.W., 2008. Middle Miocene ice sheet dynamics, deep-sea temperatures, and carbon cycling: a Southern Ocean perspective. Geochemistry, Geophysics, Geosystems 9, Q02006. Available from: https://doi.org/10.1029/2007GC001736.

Siegert, M.J., Golledge, N.R., 2021. Advances in numerical modelling of the Antarctic ice sheet. In: Florindo, F., et al., (Eds.), Antarctic Climate Evolution, second edition. Elsevier (this volume).

Siegert, M.J., Hein, A.S., White, D.A., Gore, D.B., De Santis, L., Hillenbrand, C.D., 2021. Antarctic ice sheet changes since the Last Glacial Maximum. In: Florindo, F., et al. (Eds.), Antarctic Climate Evolution, second edition. Elsevier (this volume).

Sijp, W.P., Anna, S., Dijkstra, H.A., Flögel, S., Douglas, P.M., Bijl, P.K., 2014. The role of ocean gateways on cooling climate on long time scales. Global and Planetary Change 119, 1–22.

Sorlien, C., Luyendyk, B., Wilson, D., Decesari, R., Bartek, L., Diebold, J., 2007. Oligocene development of the West Antarctic ice sheet recorded in eastern Ross Sea strata. Geology 35 (5), 467–470. Available from: https://doi.org/10.1130/G23387A.1.

Stap, L.B., Sutter, J., Knorr, G., Stärz, M., Lohmann, G., 2019. Transient variability of the Miocene Antarctic ice sheet smaller than equilibrium differences. Geophysical Research Letters 46, 4288–4298. Available from: https://doi.org/10.1029/2019GL082163.

Steinthorsdottir, M., Coxall, H.K., de Boer, A.M., Huber, M., Barbolini, N., Bradshaw, C.D., et al., 2021. The Miocene: The future of the past. Paleoceanography and Paleoclimatology 36, e2020PA004037. Available from: https://doi.org/10.1029/2020PA004037.

Steinthorsdottir, M., Vajda, V., Pole, M., 2019. Significant transient pCO_2 perturbation at the New Zealand Oligocene–Miocene transition recorded by fossil plant stomata. Palaeogeography, Palaeoclimatology, Palaeoecology 515, 152–161. Available from: https://doi.org/10.1016/j.palaeo.2018.01.039.

Stewart, J.A., James, R.H., Anand, P., Wilson, P.A., 2017. Silicate weathering and carbon cycle controls on the Oligocene–Miocene transition glaciation. Paleoceanography 32, 1070–1085. Available from: https://doi.org/10.1002/2017PA003115.

Strother, S.L., Salzmann, U., Sangiorgi, F., Bijl, P.K., Pross, J., Escutia, C., 2017. A new quantitative approach to identify reworking in Eocene to Miocene pollen records from offshore Antarctica using red fluorescence and digital imaging. Biogeosciences 14, 2089–2100. Available from: https://doi.org/10.5194/bg-14-2089-2017.

Super, J.R., Thomas, E., Pagani, M., Huber, M., O'Brien, C., Hull, P.M., 2018. North Atlantic temperature and pCO_2 coupling in the early-middle Miocene. Geology 46 (6), 519–522. Available from: https://doi.org/10.1130/G40228.1.

Tauxe, L., Stickley, C.E., Sugisaki, S., Bijl, P.K., Bohaty, S.M., Brinkhuis, H., et al., 2012. Chronostratigraphic framework for the IODP Expedition 318 Wilkes land margin: constraints for paleoceanographic reconstruction. Paleoceanography 27 (2). Available from: https://doi.org/10.1029/2012PA002308 PA2214.

Taviani, M., Beu, A.G., 2003. The palaeoclimatic significance of Cenozoic marine macrofossil assemblages from Cape Roberts Project drillholes, McMurdo Sound, Victoria Land Basin, East Antarctica. Palaeogeography, Palaeoclimatology, Palaeoecology 198 (1–2), 131–143.

Toggweiler, J.R., Russell, J.L., Carson, S.R., 2007. Mid-latitude westerlies, atmospheric CO_2, and climate change. Paleoceanography 21. Available from: https://doi.org/10.1029/2005PA001154(2007).

Watkins, D.K., Villa, G., 2000. Palaeogene calcareous nannofossils from CRP-2/2A, Victoria Land Basin, Antarctica. Terra Antarctica 7 (4), 443–452.

Westerhold, T., Marwan, N., Drury, A.J., Liebrand, D., Agnini, C., Anagnostou, E., et al., 2020. An astronomically dated record of Earth's climate and its predictability over the last 66 million years. Science 369 (6509), 1383–1387. Available from: http://doi.org/10.1126/science.aba6853.

Wilson, D.S., Luyendyk, B.P., 2009. West Antarctic paleotopography estimated at the Eocene–Oligocene climate transition. Geophysical Research Letters 36 (16).

Wilson, G.S., Lavelle, M., McIntosh, W.C., Roberts, A.P., Harwood, D.M., Watkins, D.K., et al., 2002. Integrated chronostratigraphic calibration of the Oligocene–Miocene boundary at 24.0 ± 0.1 Ma from the CRP-2A drill core, Ross Sea, Antarctica. Geology 30, 1043–1046.

Wilson, G.S., Pekar, S.F., Naish, T.R., Passchier, S., DeConto, R., 2009. The Oligocene-Miocene Boundary—Antarctic Climate Response to Orbital Forcing. In: Florindo, F., Siegert, M. (Eds.), Developments in Earth and Environmental Sciences, Vol. 8: Antarctic Climate Evolution. Elsevier, Amsterdam, pp. 369–400.

Wilson, D.S., Pollard, D., DeConto, R., Jamieson, S.S.R., Luyendyk, B.P., 2013. Initiation of the West Antarctic ice sheet and estimates of total Antarctic ice volume in the earliest Oligocene. Geophysical Research Letters 40 (16), 4305–4309.

Witkowski, C.R., Weijers, J.W., Blais, B., Schouten, S., Sinninghe Damsté, J.S., 2018. Molecular fossils from phytoplankton reveal secular pCO_2 trend over the Phanerozoic. Science Advances 4 (11), eaat4556.

Zachos, J.C., Flower, B.P., Paul, H., 1997. Orbitally paced climate oscillations across the Oligocene/Miocene boundary. Nature 388 (6642), 567–570. Available from: https://doi.org/10.1038/41528.

Zachos, J., Pagani, M., Sloan, L., Thomas, E., Billups, K., 2001a. Trends, rhythms, and aberrations in global climate 65 Ma to present. Science 292 (5517), 686–693. Available from: https://doi.org/10.1126/science.1059412.

Zachos, J.C., Shackleton, N.J., Revenaugh, J., Pälike, H., Flower, B.P., 2001b. Climate response to orbital forcing across the Oligocene–Miocene boundary. Science 292, 274–278.

Zhang, Y.G., Pagani, M., Liu, Z., Bohaty, S.M., DeConto, R.M., 2013. A 40-million-year history of atmospheric CO_2. Philosophical Transactions of the Royal Society A 371, 20130096. Available from: https://doi.org/10.1098/rsta.2013.0096.